Cellular senescence in facial senile lentigo

JID Open

Journal of Investigative Dermatology (2026) ■, ■–■; doi:10.1016/j.jid.2026.04.024

TO THE EDITOR

Senescent, terminally growth-arrested, cells have been widely reported to accumulate in various organs during the aging process, contributing to functional and structural deterioration through the disruption of tissue homeostasis and the senescence-associated secretory phenotype. In the dermal and epidermal layers of the skin, various manifestations of aging have been associated with an accumulation of senescent cells, namely fibroblasts, keratinocytes, and melanocytes (Chin et al, 2023; Ogrodnik et al, 2024). We and others have previously reported an accumulation of senescent cells in chronologically aged epidermis upon exposure to chronic low-dose UV radiation and in the epidermis of precancerous actinic keratosis, age-associated lesions that frequently occur in sun-damaged skin (Wang et al, 2022). Since the prevalence of photoaging in Asian populations commonly results in skin hyperpigmentation, we here extended our investigation to senile lentigo (SL), a common age-associated hyperpigmentation disorder caused by chronic UV exposure. Previous studies have reported an increased accumulation of $p16^{INK4A}$-positive senescent fibroblasts in the dermis of SL lesions (Yoon et al, 2018), as well as during chronological skin aging (Kim et al, 2022). However, the dynamic nature of senescence necessitates the use of multiple biomarkers to reliably detect senescent cells in complex tissues such as the skin (Ogrodnik et al, 2024). Thus, in this study, we characterized isogenic perilesional and lesional skin of SL using a combination of morphological hallmarks, pigmentation, senescence- and proliferation-associated biomarkers, including H&E and Fontana-Masson staining, epidermal thickness, TRP1 (melanocytes), Ki-67 (proliferation), lamin B1, $p16^{INK4A}$ and nuclear size (senescence hallmarks). This analysis revealed an accumulation of cells exhibiting characteristics of cellular senescence within the SL epidermis. To investigate the functional relevance of these findings, we conducted melanocyte: keratinocyte co-culture experiments and demonstrated that the presence of senescent keratinocytes stimulates pigment production, transport, and accumulation in keratinocytes, thereby providing functional evidence linking senescent cell populations to the persistence of SL.

Facial skin biopsy samples from 9 donors of Korean ethnicity, classified under type III or IV on the Fitzpatrick scale, were collected from both perilesional and lesional sites. Expectedly, we observed a higher degree of pigmentation and more melanocytes (as indicated by an increased number of TRP1-positive cells in proportion to epidermal length) within SL lesions (Figure 1). In addition, quantification of H&E and immunofluorescent Ki-67 staining revealed an epidermal thickening in lesional skin compared to adjacent non-lesional control skin. Although statistically insignificant, the overall trend agrees with previous data showing localized thickening of the SL epidermis (Shin et al, 2015). To determine whether SL lesions are associated with an accumulation of senescent cells, we stained sections for well-characterized hallmarks of senescence: $p16^{INK4A}$, lamin B1, and increased nuclear size. This analysis revealed increased nuclear $p16^{INK4A}$ staining in the basal layer and more diffuse staining in the suprabasal layer in lesional epidermis compared to perilesional epidermis (Figure 1). In addition, we found an accumulation of cells with reduced lamin B1 levels and significantly enlarged nuclei in lesional epidermis, including the keratin 10-positive suprabasal layer (Supplementary Figure S1), which are not found in proliferating or $CaCl_2$-induced differentiating keratinocytes (Figure 1; Supplementary Figure S2a–e).

To investigate the potential functional relevance of these findings, we conducted co-culture experiments of senescent versus proliferating control keratinocytes and melanocytes. Keratinocyte senescence was induced by treating N/TERT or primary keratinocytes with etoposide (ETOP) for 48 hours. Four days post treatment, senescent or proliferating control keratinocytes were co-cultured with melanocytes at a ratio of 10:1, as previously described (Figure 2a) (Phua et al, 2023). Senescence induction, melanin production, and accumulation in keratinocytes were quantified 24 hours later by SA-β-gal staining, melanin assay, RT-PCR, and quantitative immunofluorescence microscopy, respectively. As shown in Figure 2b and c, etoposide treatment resulted in the generation of homogeneous populations of senescent keratinocytes, as previously described (Yosef et al, 2016). The presence of senescent primary or N/TERT keratinocytes stimulated melanin production (Figure 2d, Supplementary Figure S2f), increased the accumulation of glycoprotein 100+ granules in K14+ senescent keratinocytes (Figure 2e and f), and increased the expression of melanogenesis and melanin transport regulators (Figure 2g). Collectively, these results suggest that the accumulation of senescent cell populations with a high melanin burden contributes to the persistence of SL. These findings may also support the notion that SL can progress toward seborrheic keratosis.

Our previous report showed an accumulation of $p16^{INK4A}$-positive senescent fibroblasts in the dermis of SL lesions, and senescent fibroblasts have been shown to stimulate increased melanin production in melanocytes (Yoon et al, 2018). Another study suggested that senescent melanocytes are a main contributor to biological skin aging (Victorelli et al, 2019). However, these insightful studies relied on a single marker approach to detect senescent cells ($p16^{INK4A}$) and may not fully capture the dynamic state of senescence

Abbreviation: SL, senile lentigo

Accepted manuscript published online XXX; corrected proof published online XXX

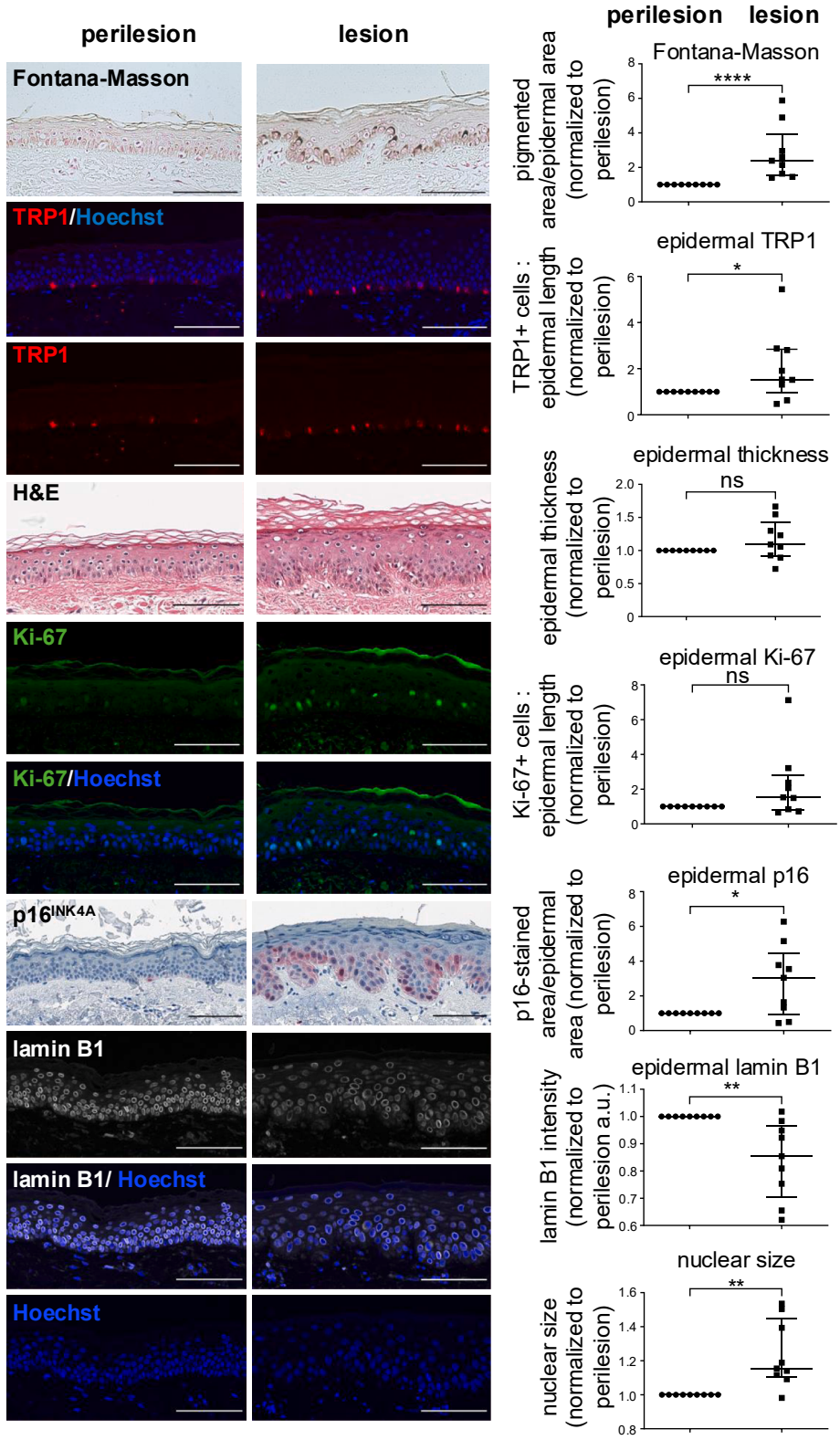

Figure 1. Characteristic hallmarks of solar lentigo perilesional versus lesional skin. Left panels: FM and H&E staining, immunofluorescence staining against TRP1 (Santa Cruz, sc166857) and Ki-67 (Agilent Technologies, m7240) and respective nuclear stain (Hoechst). Immunohistochemistry and immunofluorescence staining of senescence biomarkers $p16^{INK4A}$ and lamin B1, respectively, in perilesional (left) versus lesional (right) skin samples. Nuclear stain (Hoechst) is shown for lamin B1. Right panels: Quantification of FM (pigmented area per epidermal area was measured). TRP1-positive cells, epidermal thickness, and Ki-67-positive cells are indicated. Quantifications of $p16^{INK4A}$ (Roche, 805−4713), lamin B1 (Proteintech, 12987-1-AP), and nuclear size are indicated (n = 9). The mean with SD is plotted with the individual dots showing the averages of each set. Mann-Whitney test: **** = < .0001, ** = .0019, * = .0361, ns; scale bar = 100 μm. FM, Fontana-Masson; ns, not significant.

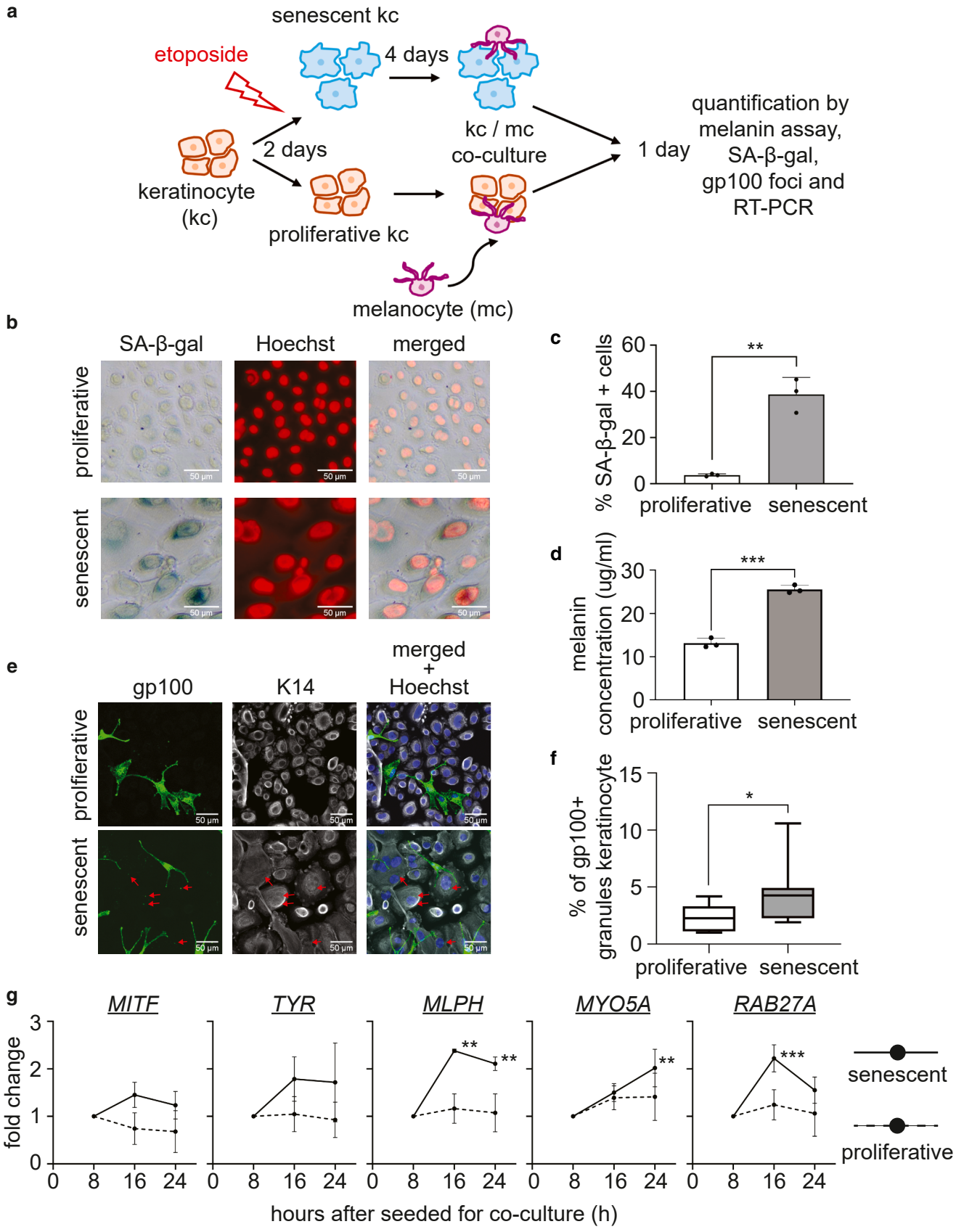

Figure 2. Senescent keratinocytes stimulate melanin production in keratinocyte: melanocyte co-culture model. (**a**) Schematic representation of experimental design. Proliferating control or ETOP-induced senescent N/TERT keratinocytes were co-cultured with melanocytes. Melanin assay and senescence validation (via SA-β-gal) was conducted 24 hours post co-culture. **(b)** SA-β-gal staining of keratinocyte: melanocyte co-cultures (upper panel: proliferative control; lower panel: senescent). 5 μM ETOP was used to induce senescence. Hoechst staining is displayed in red. Size markers: 50 μm. **(c)** Quantification of SA-β-gal-positive

in different skin cell types and age-related pathologies. Here, we used a combination of senescence biomarkers (lamin B1, $p16^{INK4A}$ and nuclear size measurement) and found an accumulation of senescent cells in SL epidermis. This is of particular interest because we and others have previously observed an accumulation of senescent keratinocytes in actinic keratosis lesions and in chronically UV-exposed skin (Wang et al, 2017, 2022). Moreover, it is noteworthy that patients with Hutchinson-Gilford progeria, a premature aging syndrome caused by an altered form of lamin A that triggers cellular senescence, exhibit widespread hyper- as well as hypopigmentation. However, the extent to which different cell types within the skin contribute to this phenotype remains unclear. Importantly, while the senescence-associated secretory phenotype in senescent human fibroblasts is well characterized, very little is known about the senescence-associated secretory phenotype in keratinocytes. Further mechanistic studies will be required to investigate the impact of different senescent skin cell types on their non-senescent counterparts. These experiments will lay the foundation to investigate whether topical treatment with senolytic or senomorphic agents may ameliorate age-related skin manifestations.

ETHICS STATEMENT

This study was conducted in accordance with the principles of the Declaration of Helsinki. Approval was obtained from the Institutional Review Board (AJOUIRB-MDB-2021-068) at Ajou University Hospital. Written informed consent was obtained from all participants prior to their inclusion in this study.

DATA AVAILABILITY STATEMENT

The authors affirm that all other data necessary for confirming the conclusions of the article are present within the article and its figures.

KEYWORDS

Epidermis; Keratinocytes; Pigmentation; Senescence; Senile lentigo

ORCIDs

Mattheus Xing Rong Foo: http://orcid.org/0000-0002-7476-2249
Tristy Abigayle Marta: http://orcid.org/0009-0006-1701-6318
Yul Hee Kim: http://orcid.org/0000-0003-3589-8896
Xin Er Lee: http://orcid.org/0000-0002-7413-7603
Du Jin Baek: http://orcid.org/0000-0002-5356-6716
Selwyn Jun Xi Low: http://orcid.org/0000-0002-7397-5672
Yeongeun Kim: http://orcid.org/0000-0002-6113-1253
Hee Young Kang: http://orcid.org/0000-0001-8697-4292
Oliver Dreesen: http://orcid.org/0000-0003-1148-3557

CONFLICTS OF INTEREST

The authors state no conflict of interest.

ACKNOWLEDGMENTS

We acknowledge the support from the A*STAR Microscopy Platform. This project is supported by the RIE2025 Human Health and Potential (HHP) industry alignment fund pre-positioning (IAF-PP) Grant number H24J4a0003, administered by the Singapore Agency for Science, Technology (A*STAR). Guarantor for this article is Oliver Dreesen.

AUTHOR CONTRIBUTIONS

Conceptualization: HYK, OD; Data Curation: MXRF, TAM, YHK, XEL, DJB, HYK, OD; Investigation: MXRF, TAM, YHK, XEL, SJXL, YK; Methodology: MXRF, TAM, YHK, XEL, HYK, OD; Project Administration: HYK, OD; Supervision: HYK, OD; Validation: MXRF, TAM, YHK, XEL, DJB, SJXL, YK, HYK, OD; Visualization: MXRF, TAM, YHK, XEL, DJB, SJXL, YK, HYK, OD; Writing − Original Draft Preparation: YHK, XEL, HYK, OD; Writing − Review and Editing: MXRF, TAM, HYK, OD

DECLARATION OF GENERATIVE ARTIFICIAL INTELLIGENCE (AI) OR LARGE LANGUAGE MODELS (LLMS)

The author(s) did not use AI/LLM in any part of the research process and/or manuscript preparation.

***Mattheus Xing Rong Foo*[1,4], *Tristy Abigayle Marta*[1,4], *Yul Hee Kim*[2,4], *Xin Er Lee*[1,4], *Du Jin Baek*[2], *Selwyn Jun Xi Low*[1], *Yeongeun Kim*[2], *Hee Young Kang*[2,*] and *Oliver Dreesen*[1,3,*]**

[1]*Cell Aging Laboratory, A*STAR Skin Research Labs (A*SRL), Singapore;* [2]*Department of Dermatology, Ajou University School of Medicine, Suwon, Korea; and* [3]*Mechanobiology Institute, National University of Singapore, Singapore*

[4]*Those authors contributed equally to this work.*

[*]*Corresponding author e-mails: hykang@ajou.ac.kr and oliver_dreesen@a-star.edu.sg*

SUPPLEMENTARY MATERIAL

Supplementary material is linked to the online version of the paper at www.jidonline.org, and at 10.1016/j.jid.2026.04.024.

REFERENCES

Chin T, Lee XE, Ng PY, Lee Y, Dreesen O. The role of cellular senescence in skin aging and age-related skin pathologies. Front Physiol 2023;14:1297637.

Kim TH, Park TJ, Kweon YY, Baek DJ, Lee JW, Kang HY. Age-dependent sequential increase of senescent cells in the skin. J Invest Dermatol 2022;142:2521−3.e1.

Ogrodnik M, Carlos Acosta J, Adams PD, d'Adda di Fagagna F, Baker DJ, Bishop CL, et al. Guidelines for minimal information on cellular senescence experimentation in vivo. Cell 2024;187:4150−75.

Phua R, Tien TZ, Goh G, Pantelireis N, Sim KSH, Lim J, et al. In vitro quantification of pigment production and transfer in 2D co-cultures and 3D skin organotypic. Star Protoc 2023;4:102334.

Shin J, Park JY, Kim SJ, Kang HY. Characteristics of keratinocytes in facial solar lentigo with flattened rete ridges: comparison with melasma. Clin Exp Dermatol 2015;40:489−94.

Victorelli S, Lagnado A, Halim J, Moore W, Talbot D, Barrett K, et al. Senescent human melanocytes drive skin ageing via paracrine telomere dysfunction. EMBO J 2019;38.

Wang AS, Nakamizo S, Ishida Y, Klassen G, Chong P, Wada A, et al. Identification and quantification of senescent cell types by lamin B1 and HMGB1 in actinic keratosis lesions. J Dermatol Sci 2022;105:61−4.

Wang AS, Ong PF, Chojnowski A, Clavel C, Dreesen O. Loss of lamin B1 is a biomarker to quantify cellular senescence in photoaged skin. Sci Rep 2017;7:15678.

Yoon JE, Kim Y, Kwon S, Kim M, Kim YH, Kim JH, et al. Senescent fibroblasts drive ageing pigmentation: a potential therapeutic target for senile lentigo. Theranostics 2018;8:4620−32.

Yosef R, Pilpel N, Tokarsky-Amiel R, Biran A, Ovadya Y, Cohen S, et al. Directed elimination of senescent cells by inhibition of BCL-W and BCL-XL. Nat Commun 2016;7:11190.

cells. Student's *t*-test was conducted (** < .01, n = 3). **(d)** Quantification of melanin (mg/ml) from 200,000 cells of proliferating versus senescent co-cultures. 20 μM ETOP was used for senescence induction. Student's *t*-test was conducted (*** < .001, n = 3). **(e)** gp100 and K14 immunofluorescence confocal imaging of keratinocyte: melanocyte co-cultures (upper panel: proliferating control; lower panel: senescent). 20 mM ETOP was used for senescence induction. Size markers: 50 μm. **(f)** Percentage of gp100 granules in K14+ keratinocytes. K14+ keratinocytes were considered gp100+ when the gp100 granules were within 4 μm of the nucleus. Student's *t*-test was conducted (* < .05, n = 7). g) RT-PCR quantification of indicated genes within 24 hours of co-culture. Values were normalized to the 8-hour timepoint. 5 μM ETOP was used for senescence induction. Two-way ANOVA with Bonferroni's posttest was performed (comparison was done against the 8-hour timepoint, ** < .01, *** < .001, n =3 for *MITF, TYR, MYO5A* and *RAB27A*, n = 2 for *MLPH).* ETOP, etoposide; gp100, glycoprotein 100, K, keratin.

SUPPLEMENTARY MATERIALS

Cell culture

The N/TERTs, primary keratinocytes, primary melanocytes, and human dermal fibroblasts were obtained from the Rheinwald lab (CVCL_CW92, Brigham and Women's Hospital, USA), the Asian Skin Biobank (A*STAR, Singapore), Thermo Fisher Scientific (USA), and the Reversade lab (A*STAR, Singapore), respectively. N/TERTs and primary keratinocytes were grown in a Dermalife-K complete kit (Lifeline Cell Technology, LL-0007), while primary melanocytes were cultured in Medium 254 (Life Technologies, M-254-500) with HMGS2 (Life Technologies, S-016-5). Fibroblasts were grown in minimum essential medium (Invitrogen, 10370088) supplemented with 2 mM glutamine (Invitrogen, 25030081-P), 15% fetal bovine serum (Invitrogen, SH30071.03), and 50 U/ml Penicillin-Streptomycin (Invitrogen, 15140122). To passage keratinocytes and fibroblasts, cells were incubated in 0.25% Trypsin with EDTA (Life Technologies, 25200056) for 3 minutes, while subculturing of melanocytes used 0.05% Trypsin with EDTA (Pan Biotech, Germany, PAB. P10-0231SP) for 3 minutes. Trypsin was neutralized with 10% fetal bovine serum in dPBS. For co-culture experiments, melanocyte medium (stated above) was used, and 0.25% Trypsin with EDTA was used for 5 minutes (for passaging). Etoposide (Afirmus Biosource Pte Ltd, Singapore) and $CaCl_2$ concentrations are indicated in the respective figure legends.

Keratinocyte: melanocyte co-culture

The keratinocyte: melanocyte co-culture procedure is illustrated in Figure 2a and described by Phua et al (2023). Briefly, keratinocytes were treated with etoposide (or DMSO control) for 2 days. Four days later, treated keratinocytes and primary melanocytes were trypsinized and mixed at a 10:1 ratio. For RT-PCR, control keratinocytes were treated with etoposide for 4 hours instead of DMSO just before trypsinization to prevent proliferation during the co-culture. Co-cultures were processed for melanin assay or immunofluorescence ~24 hours later, or for RT-PCR at 8-, 16-, and 24-hour timepoints.

RT-PCR

Total RNA was harvested from co-cultures with Arcturus PicoPure RNA Isolation Kit (Life Technologies) and RNase-Free DNase Set (Qiagen). The RNA was converted to cDNA using iScript Reverse Transcription Supermix (Bio-Rad) at 42 °C for 30 minutes, including a no-RT control. 10 ng of cDNA mixed with 500 nM of primers and 1 × iTaq Universal SYBR Green Supermix (Bio-Rad) before being loaded into a MicroAmp Optical 384-Well Reaction Plate. The no-RT samples and a no-template condition were added for quality control as well. The primer sequences used are listed below:

- *ACTB* (Length: 97 bp)
  F: CCA ACC GCG AGA AGA TGA
  R: CCA GAG GCG TAC AGG GAT AG
- *MITF* (Length: 170 bp)
  F: AGA ACA GCA ACG CGC AAA AGA AC
  R: TGA TGA TCC GAT TCA CCA AAT CTG
- *TYR* (Length: 134 bp)
  F: CAC CAC TTG GGC CTC AAT TTC
  R: AAA GCC AAA CTT GCA GTT TCC AC
- *MYO5A* (Length: 435 bp)
  F: AGT CTC TGT GTC GTT CAT TCG
  R: CCT GTA TGT AAA CTC ACG GTA
- *RAB27A* (Length: 77 bp)
  F: TGG AGG ACC AGA GAG TAG TGA AA
  R: AGT TTC AAA GTA GGG GAT TCC A
- *MLPH* (Length: 284 bp)
  F: GCC CAT CAA ACC AAC AGA CA
  R: TCC TCT GGT CTC TTG CCA AG

RT-PCR was conducted using the QuantStudio 5 Real-Time PCR System (Thermo Fisher Scientific) and melt curve analysis was performed with Diomni Design and Analysis (RUO) Software. To calculate the relative RNA expression fold change, the ΔΔCq calculation method (normalized to β-actin and the 8-hour time point) was used.

Melanin assay

The total amount of melanin within co-cultures was quantified using the protocol described by Phua et al (2023) in 2023. Briefly, co-cultures were trypsinized, cells were counted, and 200,000 or 50,000 cells (as indicated in the legends) were lysed with cOmplete Lysis-M EDTA-free kit and cOmplete Protease Inhibitor Cocktail (Roche, Switzerland). Lysates were spun down at 14,000 r.p.m for 10 minutes with a tabletop centrifuge, and the supernatant was transferred to a separate tube. This supernatant was spun again at 14,000 r.p.m for 10 minutes, and the pellets were kept. Pellets from both spins were resuspended in 120 μl 1 M NaOH, combined, and heated at 80 °C for 1 hour, in parallel with melanin standards. Samples and standards were loaded into a 96-well Greiner clear, flat-bottom plate, and the 475 nm absorbance was quantified.

Immunofluorescence imaging

N/TERTs were either treated with etoposide, DMSO control, or $CaCl_2$ for 2 days (etoposide and $CaCl_2$ concentrations are indicated in the figure legends). Immunofluorescence staining was performed 3–4 days later. Fibroblasts were treated with etoposide for 2 days and fixed one day later. All cells, including the co-culture slides, were fixed with 2% paraformaldehyde (Precision Technologies Pte Ltd, Singapore) for 20 minutes, neutralized with 50 mM NH_4Cl for 5 minutes, permeabilized with 1% Triton X-100 (Millipore) and 0.1% SDS (Promega) for 5 minutes, blocked using 0.2% gelatin in dPBS for 10 minutes, and stained with primary antibodies overnight at 4 °C. Secondary antibodies were added the following day for at least 1 hour at room temperature. PBS washes were performed before and after each step mentioned above. Images were acquired on a confocal (FV3000RS) microscope or a widefield (Zeiss Axio Observer 7 HCS) microscope and analyzed via ImageJ (Schindelin et al, 2012).

Gp100 granule quantification in K14+ keratinocytes

To quantify gp100 granules within K14+ keratinocytes, nuclei (Hoechst) were first thresholded using ImageJ

(Schindelin et al, 2012) and the nuclear area masks were dilated 5 times to obtain an approximate 4 μm radius from the nuclear border. The function "watershed" was then performed to separate the masks and "analyze particle" was used to create the region of interest. Both K14+ and gp100+ channels were then thresholded, and gp100+ foci, ranging from 0−10 μm^2, that were within the K14+ areas were quantified. The nuclear regions of interest with at least 1 focus were counted as a gp100+ keratinocyte.

SA-β-gal

To perform SA-β-gal, keratinocyte: melanocyte co-cultures were fixed with 2% paraformaldehyde (Precision Technologies Pte Ltd) and 0.2% glutaraldehyde for 5 minutes. 2 PBS washes were done before staining the slides as previously described (Dimri et al, 1995) and subsequently visualized using a Ts2-FL inverted microscope (Nikon, Japan).

Western blot

Protein lysates of proliferating, $CaCl_2$-induced differentiated, and etoposide-induced senescent keratinocyte cultures were obtained by lysing cells with a mix of cOmplete Lysis-M EDTA-free kit (Roche), cOmplete Protease Inhibitor Cocktail (Roche), 0.1 mM Dithiothreitol (Sigma), and 2% SDS (Promega). Pierce Microplate BCA protein assay kit − Reducing Agent Compatible (Thermo Fisher Scientific) was used for protein quantification. 10 μg of protein was run on a 4−12% Bis-Tris Gel (Invitrogen), transferred onto a nitrocellulose membrane (Bio-Rad), and blocked in Intercept (PBS) Blocking Buffer (Li-COR, USA) for 1 hour before being stained with primary antibodies at 4 °C overnight. After washing 4 × 5 minutes in PBS + 0.1% tween-20 (Promega), blots were incubated with Odyssey Infrared-labelled secondary antibodies (LI-COR), followed by another 4 rounds of washing. Finally, the blots were imaged using a LI-COR Odyssey scanner.

Antibodies

For in vivo immunofluorescence imaging, the primary antibodies used were rabbit anti-human LB1 (1:400 dilution, Proteintech, 12987-1-AP), mouse anti-human Ki67 (1:200 dilution, Agilent Technologies, M7240), mouse anti-human TRP1 (1:150 dilution, Santa Cruz, sc166857), mouse anti-human $p16^{INK4A}$ (Roche), and mouse anti-human K10 (1:200, Abcam).

For in vitro immunofluorescence imaging, the primary antibodies used were rabbit anti-human LB1 (1:300 dilution, Proteintech, 12987-1-AP), mouse anti-human gp100 (1:100 dilution, Abcam, ab34165), and rabbit anti-human K14 (1:400 dilution, USA, ab181595).

For western blotting, the primary antibodies used were mouse anti-human LB1 (1:2000 dilution, Proteintech, 66095-1-Ig), rabbit anti-human involucrin (1:2000 dilution, Abcam, ab181980), mouse anti-human filaggrin (1:500 dilution, Abcam, ab218395), rabbit anti-human GAPDH (1:2000 dilution, Proteintech, 10494-1-AP), and mouse anti-human GAPDH (1:1000 dilution, Proteintech, 60004-1-Ig).

Secondary antibodies used for immunofluorescence included donkey anti-mouse Alexa Fluor 488 (Invitrogen) and donkey anti-rabbit Alexa Fluor 488 and 647 (Invitrogen) at 1:600 and 1:500 dilutions for in vitro and in vivo experiments, respectively. For western blotting, Li-COR's donkey anti-mouse IRDYE 680 and 800 (1:10000 dilution; Li-COR) and donkey anti-rabbit IRDYE 680 and 800 (1:10000 dilution; Li-COR) were used.

Statistics

GraphPad Prism (version 10, Dotamatics) was used to calculate statistics for all tests performed. The type of statistical tests is indicated in the figure legends. Means of each set were used for calculations. Figures were plotted using Microsoft Excel or GraphPad Prism. Bar graphs show the mean values with SD while the box and whisker plot show the 90^{th} and 10^{th} percentiles.

Sample collection

Ethnicity was self-reported by the participants.

SUPPLEMENTARY REFERENCE

Phua R, Tien TZ, Goh G, Pantelireis N, Sim KSH, Lim J, et al. In vitro quantification of pigment production and transfer in 2D co-cultures and 3D skin organotypic. Star Protoc 2023;4:102334.

Dimri GP, Lee X, Basile G, Acosta M, Scott G, Roskelley C, et al. A biomarker that identifies senescent human cells in culture and in aging skin in vivo. Proc Natl Acad Sci U S A 1995;92:9363−7.

Schindelin J, Arganda-Carreras I, Frise E, Kaynig V, Longair M, Pietzsch T, et al. Fiji: an open-source platform for biological-image analysis. Nat Methods 2012;9:676−82.

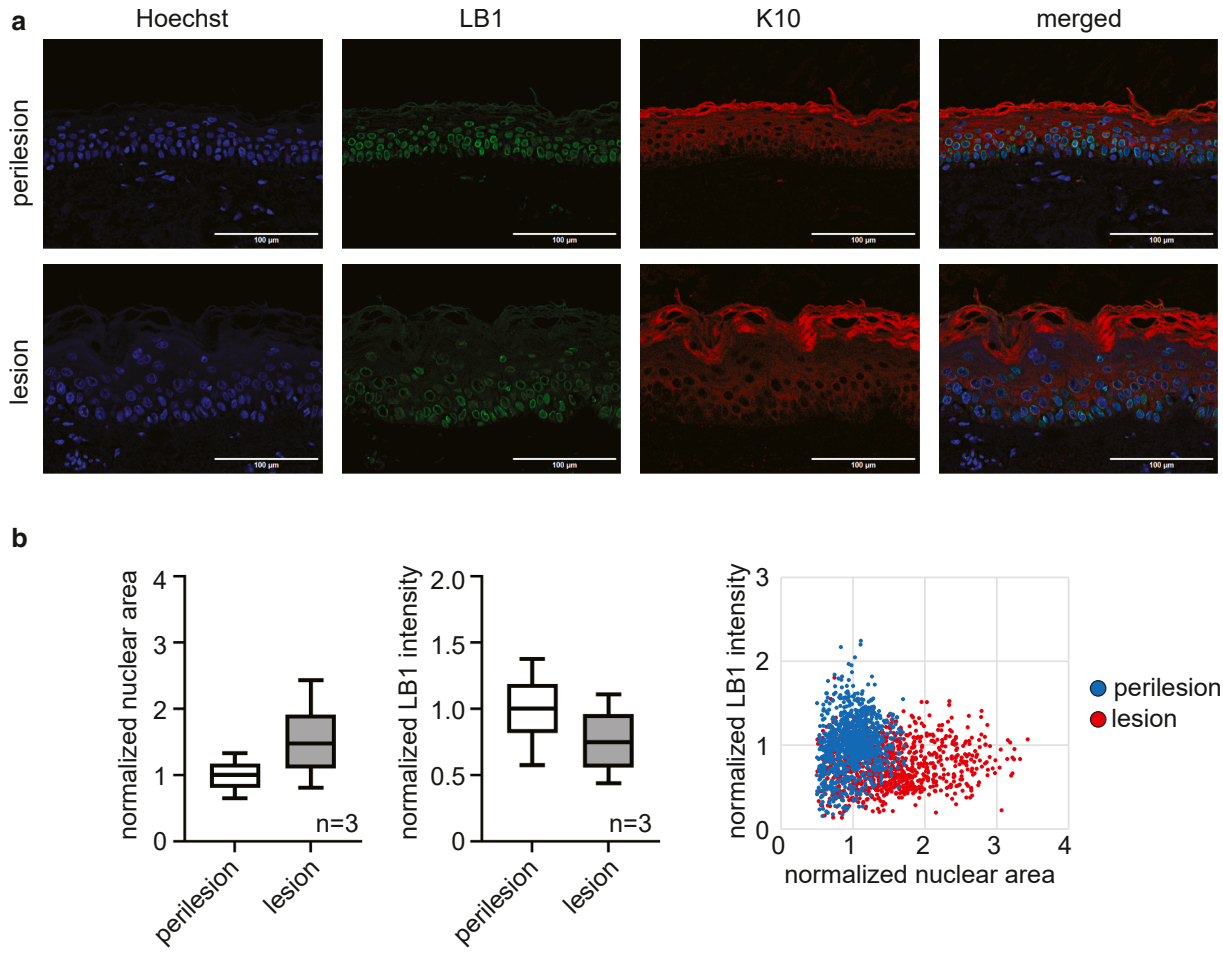

Supplementary Figure S1. (a) Immunofluorescence imaging of lamin B1 (LB1) and K10 in solar lentigo perilesional versus lesional skin (upper panel: perilesion; lower panel: lesion). Size markers: 100 µm. **(b)** Quantification of nuclear area (Hoechst) and LB1 in K10-positive perilesional versus lesional skin via confocal immunofluorescence imaging. Nuclear area and LB1 intensities were normalized to the mean of the perilesional cells. Box and whisker plot of normalized nuclear area and LB1 intensities (left and middle panels) and their representative scatter plot (right panel) are shown. Welch's t-test was performed (n = 3). K, keratin.

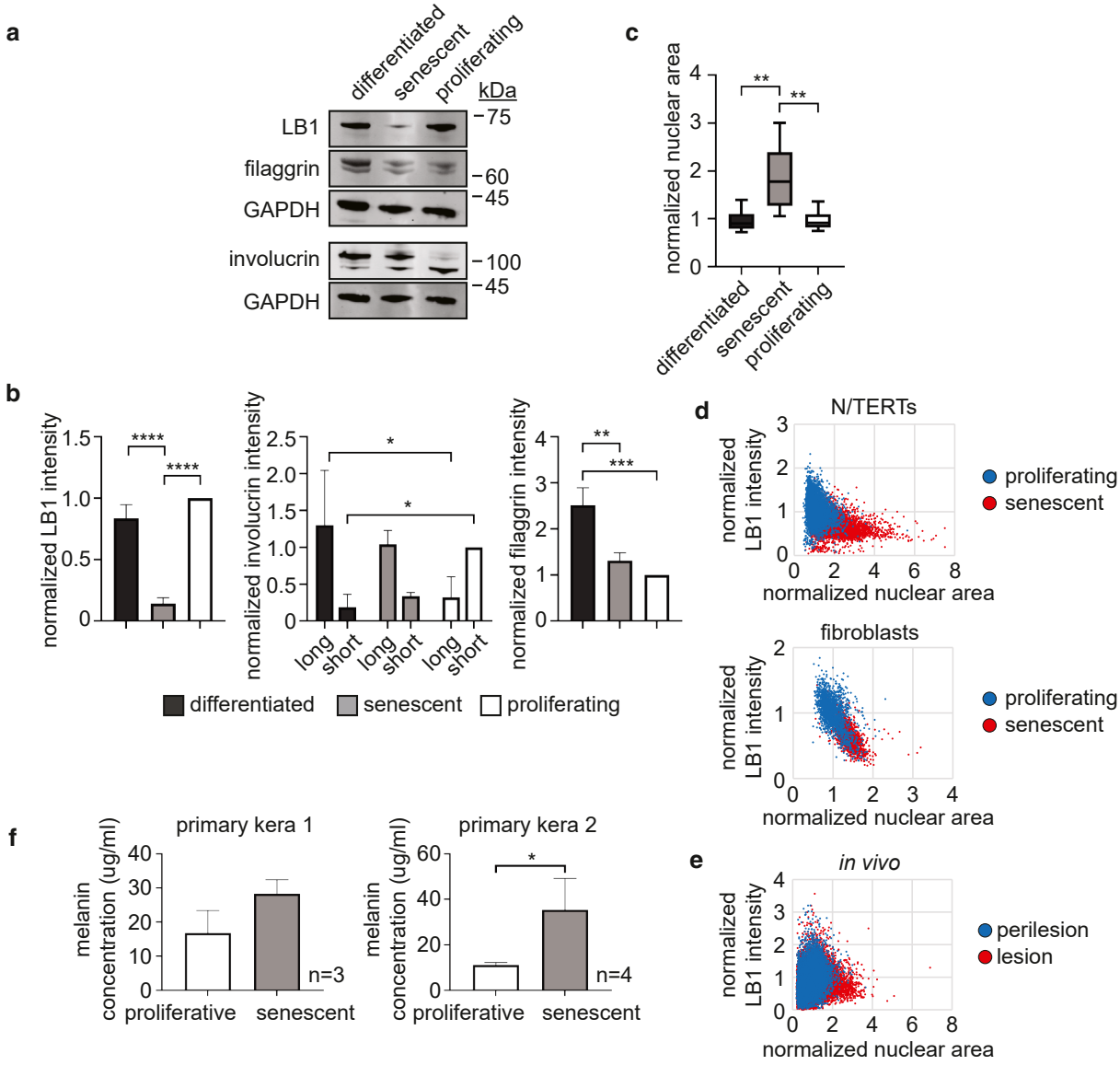

Supplementary Figure S2. (a) Representative western blot of differentiated, senescent, and proliferating N/TERT keratinocytes. LB1, filaggrin and GAPDH (upper panels) and involucrin and GAPDH (lower panels) were stained on different western blots. Cells were induced to differentiate or senesce by 1.2 mM $CaCl_2$ and 20 μM ETOP, respectively. **(b)** Quantification of LB1, filaggrin, and involucrin (long and short forms) in differentiated, senescent and proliferating N/TERTs from western blots. All values were normalized against GAPDH loading control and the mean of proliferating N/TERTs. Cells were induced to differentiate or senesce by 1.2 mM $CaCl_2$ and 20 μM ETOP, respectively. One-way ANOVA with Bonferroni's posttest was performed for LB1 and filaggrin quantification whereas two-way ANOVA with Bonferroni's posttest was performed for involucrin quantification (* < .05; ** < .01; *** < .001; **** < .0001; n = 3). **(c)** Quantification of differentiated, senescent, and proliferating N/TERT nuclear area (Hoechst) via immunofluorescence imaging. Nuclear area was normalized to the mean of proliferating keratinocytes. One way ANOVA with Bonferroni's post test was conducted (** < .01, n = 4). **(d)** Scatter plot of LB1 intensity versus nuclear area for N/TERTs and human dermal fibroblasts. LB1 intensities and nuclear area (Hoechst) were quantified by immunofluorescence imaging and normalized to the means of proliferating N/TERTs or fibroblasts. N/TERTs and fibroblasts were induced to senesce with 20 μM and 50 μM ETOP, respectively. **(e)** Scatter plot of LB1 intensity versus nuclear area for entire solar lentigo skin sections shown in Figure 1. LB1 intensities and nuclear area were normalized to the means of the perilesional region (n = 9). **(f)** Quantification of melanin (μg/ml) from 50,000 cells of proliferating versus senescent co-cultures. Two different primary keratinocytes were treated with 20 μM ETOP for senescence induction. Student's *t*-test was conducted (* < .05, n = 3 for left panel, n = 4 for right panel). ETOP, etoposide.